

Applications of Finite-Time Lyapunov Exponents to the Study of Capsize in Beam Seas

Leigh McCue*

Abstract

This paper demonstrates the use of finite-time Lyapunov exponents (FTLE) for the detection of large amplitude roll motions and capsizes. The study is conducted for a simple, single degree of freedom model of the *Edith Terkol* in regular and random beam seas. The effectiveness of the FTLE technique is qualitatively compared to a scalar ship motion metric based upon the ‘energy index (EI)’ concept used for real-time identification of quiescence.

1 Introduction

For centuries chaotic vessel motions and capsizes have resulted in lost cargo, ships, and lives. For this reason it is of the utmost importance to develop tools which can provide mariners with indicators of inclement ship motions. Lyapunov exponents provide a measure of the rate of convergence or divergence of nearby trajectories thus indicating the level of sensitivity of a system to initial conditions. They have been used to demonstrate exponentially divergent, chaotic behavior in vessel motions as demonstrated by references such as Papoulias (1987), Falzarano (1990), Spyrou (1996), Murashige and collaborators (1998a; 1998b; 2000), Arnold *et al.* (2003), and McCue and Troesch (2004; 2004; 2005).

The Lyapunov exponent, however, is defined in the limit as time approaches infinity; therefore to detect instabilities in time leading to an event, such as capsizing, the finite-time form of the Lyapunov exponent is necessary. For a system of equations written in state-space form $\dot{\mathbf{x}} = \mathbf{u}(x)$, small deviations from the trajectory can be expressed by the equation $\delta\dot{x}_i = (\partial u_i / \partial x_j) \delta x_j$ (Eckhardt & Yao, 1993). $\delta\mathbf{x}$ is a vector representing the deviation from the trajectory with components for each state variable of the system. From this, the equation for the finite-time Lyapunov exponent can be written as Equation 1 (Eckhardt & Yao, 1993).

$$\lambda_T(\mathbf{x}(t), \delta\mathbf{x}(0)) = \frac{1}{T} \log \frac{\|\delta\mathbf{x}(t+T)\|}{\|\delta\mathbf{x}(t)\|} \quad (1)$$

For a multi-dimensional state space a spectrum of finite-time Lyapunov exponents can be calculated with the same number of exponents as dimension of the state-space. Methods for computing Lyapunov exponents and finite-time Lyapunov exponents from equations of motion are well developed in the literature with details available in references such as Benettin *et al.* (1980), Wolf *et al.* (1985), and Eckhardt and Yao (1993).

In this work, the results generated via finite-time Lyapunov exponents are compared to results from a path-independent scalar ship motion metric known as the energy index (EI). The energy index, initially proposed by O’Reilly (1987), is an experimentally-tested, empirically-based indicator of quiescent periods suitable for sea-based aviation operations in which an energy-like scalar value is used as a measure of ship motions (O’Reilly, 1987; Ferrier & Manning, 1998; Ferrier *et al.*, 2000a; Ferrier *et al.*, 2000b).

While it is desirable for current ship-air operations to indicate motions in all six degrees of freedom, particularly vertical accelerations (Colwell, 2002b), this study compares finite-time Lyapunov exponents to a simple formulation of the energy index based upon the two state space variables considered in this work, namely roll and roll velocity. The intention of this work is to demonstrate the capabilities of FTLE algorithms for detecting instabilities without the dependence more complicated energy index algorithms have upon empirically defined coefficients (Ferrier & Manning, 1998).

It should be clear, however, that this is not the traditional use of the energy index, rather that the energy index concept in this case is being used as a benchmark. Because the energy index has been experimentally tested and shown to accurately indicate regions of quiescence (O’Reilly, 1987), it provides a useful comparison for this proof-of-concept study. This work aims to illustrate that a mathematical approach, such as the FTLE, can

*Aerospace and Ocean Engineering, Virginia Tech, mccue@vt.edu

yield as much, or greater information into the fundamental physics driving the motions of the system to capsize or quiescence, than a method with ship and condition-dependent parameters.

2 Regular Seas

2.1 Regular seas: modelling details

For the study presented in this work, the simple single degree of freedom roll model for the *Edith Terkol* established by Soliman and Thompson (1991) and given in Equation 2 was simulated.

$$\ddot{\phi} + b_1\dot{\phi} + b_2|\dot{\phi}|\dot{\phi} + c_1\phi + c_2|\phi|\phi + c_3\phi^3 + c_4|\phi|\phi^3 + c_5\phi^5 = \frac{M(t)}{I} + \frac{W_M}{I} \quad (2)$$

In Equation 2, b_i and c_i terms are linear and nonlinear damping and stiffness coefficients respectively with specific values: $b_1 = 0.0043$, $b_2 = 0.0225$, $c_1 = 0.384$, $c_2 = 0.1296$, $c_3 = 1.0368$, $c_4 = -4.059$, $c_5 = 2.4052$, $I = 1174$, and $W_M = 0$ (Soliman & Thompson, 1991). The term $M(t)$ in regular seas is defined by Equation 3 (Senjanović *et al.*, 2000), where α_0 , the effective wave slope, is taken to equal 0.73 (Francescutto & Serra, 2002; Gu, 2004), ω_n and ω_e equal 0.62 and 0.527 rad/s respectively (Soliman & Thompson, 1991), and the terms $H = 4.94\text{m}$ and $\lambda = 221.94\text{m}$ are chosen to be consistent with results published by Soliman and Thompson in which interesting behavior is detected (1991). The general form of Equation 3 is widely available in the literature (Nayfeh & Khdeir, 1986; Nayfeh & Sanchez, 1990). Each simulation was allowed to run for 100 wave encounters or to the point of capsize. For the purposes of this work capsize was defined as exceeding the vessel's angle of vanishing stability, $\phi_v = 0.88$ rad (Soliman & Thompson, 1991).

$$M(t) = I\alpha_0\omega_n^2\pi\frac{H}{\lambda}\sin\omega_e t \quad (3)$$

2.2 Regular seas: finite-time Lyapunov exponents

Finite-time Lyapunov exponents were calculated via simulation for the numerical model of the *Edith Terkol* given by Equations 2-3. Particular attention was paid to the values and timing of maxima in the FTLE time series. Figure 1 presents histograms illustrating the values of maximum FTLE values for both capsize (top) and non-capsize (bottom) cases. Additionally, by consideration of the middle

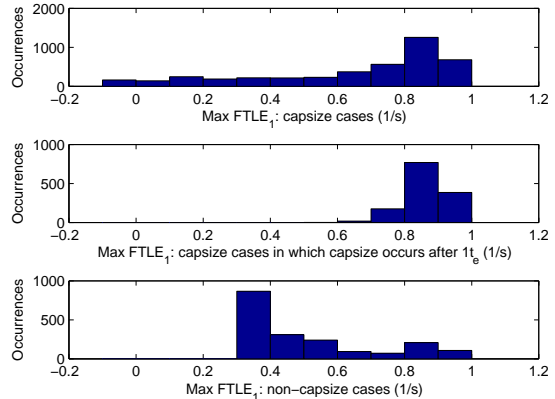


Figure 1: Histograms of maximum $FTLE_1$ for capsize and non-capsize cases in regular seas.

panel of Figure 1, it is apparent that those capsize cases with small FTLE values correspond to cases which capsize within one excitation cycle, *i.e.* those runs which capsize, for all practical purposes, immediately. Figure 2 illustrates that elimination of those cases which capsize prior to one wave cycle essentially results in removal of the cases at the extrema of roll and roll velocity initial conditions.

To demonstrate that instabilities are detectable in a time frame suitable for corrective measures to be taken, Figure 3 presents histograms of the number of wave cycles encountered between the occurrence of the maximum FTLE to the actual time of capsize. Again, the top panel includes all capsize runs while the bottom panel is restricted to those runs which capsize after one wave period. Considering only those runs which capsize after one encounter cycle, the majority capsize more than half a wave cycle after the maximum FTLE, with many capsizing multiple cycles after the location of the maxima. Detecting trends towards increasing values prior to the occurrence of maxima could lead to even greater time windows in which stabilizing controls changes are executed. This is discussed further in Section 2.3.

2.3 Regular seas: finite-time Lyapunov exponents in comparison to the energy index

For the single degree of freedom model, a simple definition of the energy index (EI) was used as given in Equation 4 (O'Reilly, 1987). Equation 4 emulates the form of the equation for the EI of O'Reilly's for motions in multiple degrees of

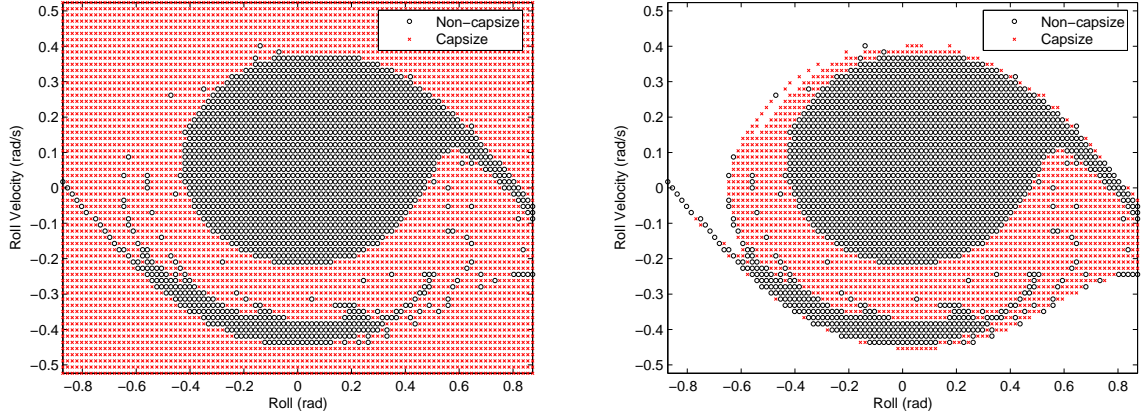


Figure 2: Safe basins indicating non-capsize and capsizing for all cases (left) and those cases capsizing after one excitation period (right) in regular seas.

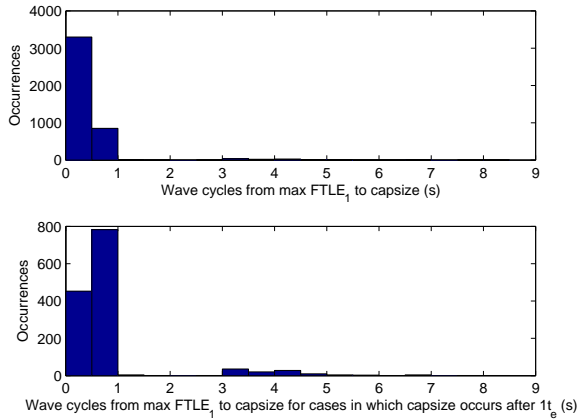


Figure 3: Histograms of wave encounter cycles from the occurrence of the maximum $FTLE_1$ to the time of capsizing in regular seas.

freedom (O'Reilly, 1987). More complicated EI models exist which rely upon empirically determined weighting coefficients for each degree of freedom (Ferrier & Manning, 1998; Ferrier *et al.*, 2000a; Ferrier *et al.*, 2000b). The purpose of this research is to demonstrate the ability to warn of large amplitude motions without a reliance upon empirical coefficients, thus justifying the use of the definition in Equation 4.

$$EI = \sqrt{\phi^2 + \dot{\phi}^2} \quad (4)$$

Figure 4 presents a comparison of roll, FTLE, and EI values for a single ship motion simulation of the *Edith Terkol* with initial conditions $(\phi \text{ rad}, \dot{\phi} \text{ rad/s}) = (0, -0.2269)$. While the energy

index reflects the instantaneous behavior of the system, the FTLE time series exhibits odd behavior, deviating from a fairly regular periodic response, 20 seconds prior to capsizing and encounters peak values one cycle before capsizing. Of particular interest is the middle plot, which displays the sum of the two FTLE for an entropy rate-like measure (Falkovich & Fouxon, 2004). Specifically, one cycle prior to capsizing, this value rises above zero.

Similar behavior is identified when examining a range of capsizing and non-capsizing cases in Figure 5 which present simulations near to the initial conditions of Figure 4. Those cases leading to capsizing begin to exhibit unique FTLE time series behavior multiple cycles prior to capsizing in addition to phase differences and peaks relative to the non-capsizing runs. Additionally, phase differences in the FTLE time series are present in the non-capsizing runs as time progresses. Some runs experience increasing roll motions while others encounter decreasing motions.

Based upon this model, there is promise that measurement of these differences and detection of peaks can indicate variations in magnitude of ship motion in addition to capsizing. Quantitatively, consideration of the sum of the FTLE values for those neighboring capsizing and non-capsizing cases in Figure 5 indicates that all capsizing cases have positive FTLE sums and non-capsizing cases have negative FTLE sums. A summary of initial conditions and values of peak $FTLE_1 + FTLE_2$ displayed in Figure 5 is as follows: $(\phi \text{ rad}, \dot{\phi} \text{ rad/s}, FTLE_1 + FTLE_2 \text{ 1/s}) = (0, -0.2618, 0.0025), (0, -0.2443, 0.0012), (0, -0.2269, 5.1439e - 004), (0, -0.2094, -0.0030), (0, -0.1920, -0.0041), (0, -0.1745, -0.0049)$.

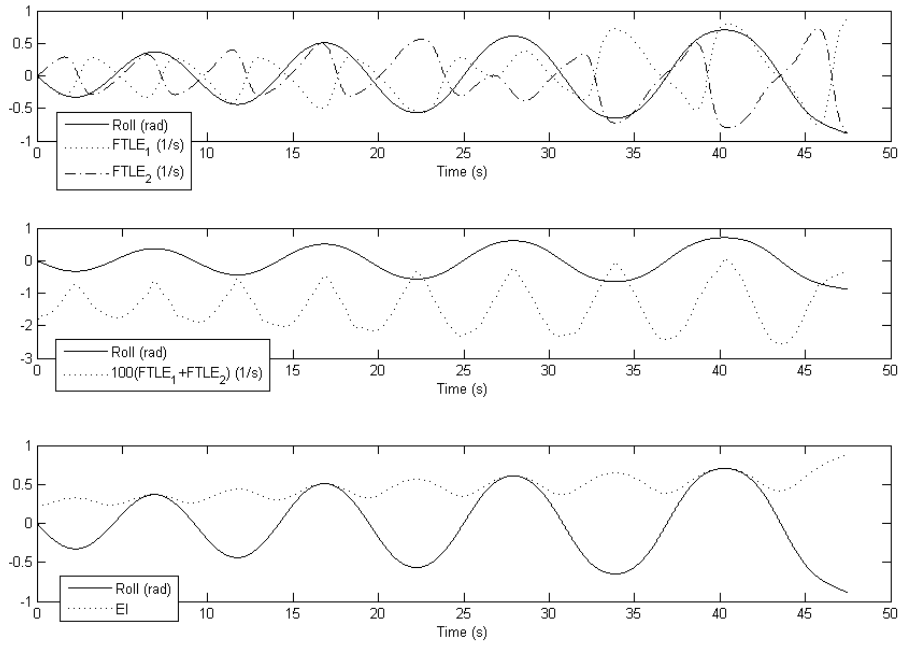


Figure 4: Roll plotted with first and second FTLE (top), sum of FTLE (middle), and EI (bottom) for *Edith Terkol* in regular beam seas, $\phi_0 = 0$ rad, $\dot{\phi}_0 = -0.2269$ rad/s.

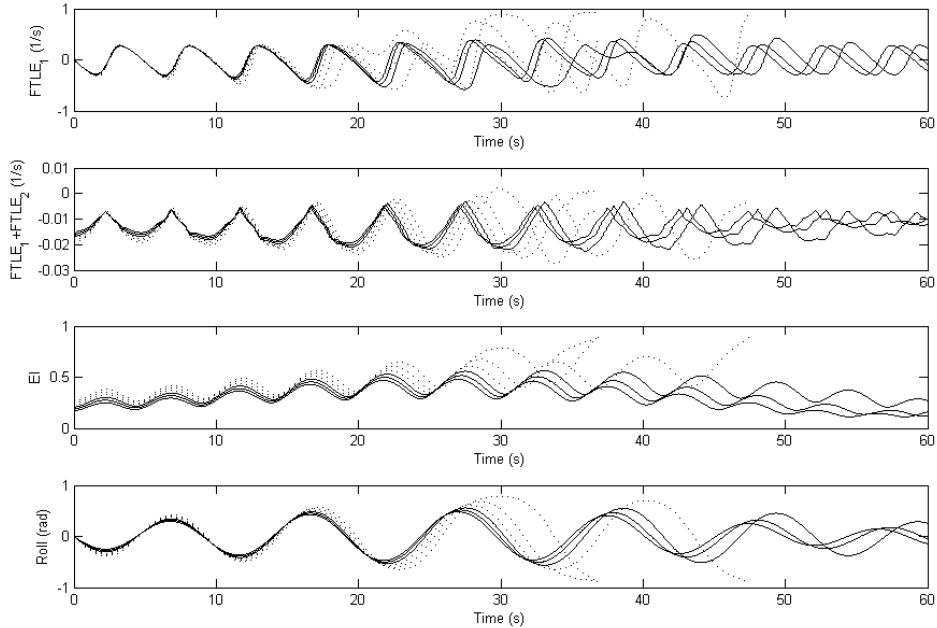


Figure 5: $FTLE_1$ (top), sum of FTLE (middle top), EI (middle bottom), and roll (bottom) for *Edith Terkol* in regular beam seas. Six cases shown corresponding to initial conditions: $\phi_0 = 0$ rad, $\dot{\phi}_0 = -0.2618$ rad/s; $\phi_0 = 0$ rad, $\dot{\phi}_0 = -0.2443$ rad/s; $\phi_0 = 0$ rad, $\dot{\phi}_0 = -0.2269$ rad/s; $\phi_0 = 0$ rad, $\dot{\phi}_0 = -0.2094$ rad/s; $\phi_0 = 0$ rad, $\dot{\phi}_0 = -0.1920$ rad/s; $\phi_0 = 0$ rad, $\dot{\phi}_0 = -0.1745$ rad/s. Dotted and solid lines denote capsizing and non-capsizing runs respectively.

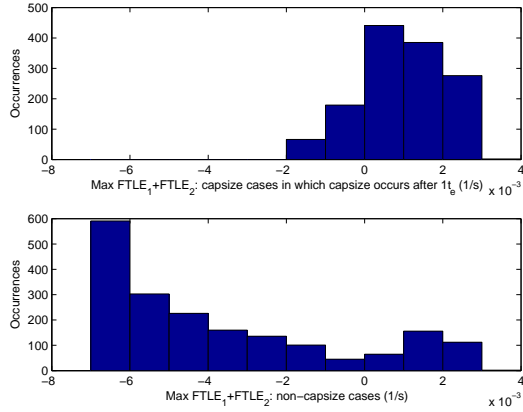


Figure 6: Histograms of maximum $FTLE_1 + FTLE_2$ for capsize and non-capsizing cases in regular seas.

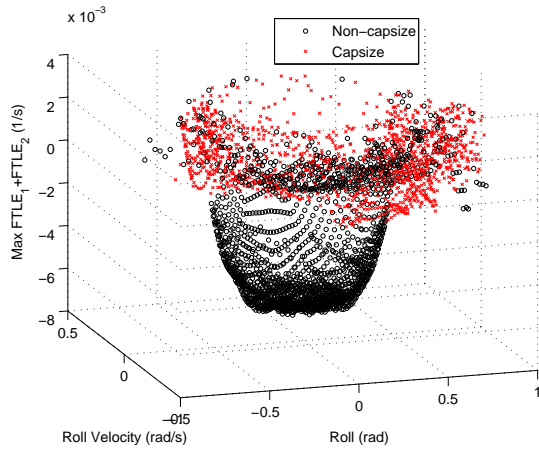


Figure 7: 3-dimensional plot of initial conditions and maximum $FTLE_1 + FTLE_2$ for capsize and non-capsizing cases in regular seas.

Figure 6 shows the range of values for maximum $FTLE_1 + FTLE_2$ for non-capsizing cases and those capsize cases in which capsizing occurs after one excitation period. The mean value for capsize cases is 0.00098 (1/s) while the mean value for non-capsizing cases is -0.0037 (1/s). Positivity of the entropy rate-like value $FTLE_1 + FTLE_2$ is an indicator of potential danger. As apparent in Figure 7, those non-capsizing runs with positive values for peak $FTLE_1 + FTLE_2$ represent simulations in the regions of greatest sensitivity to initial conditions. Thus, in addition to those areas resulting in capsizing, it is not illogical to identify such conditions as necessitating precautionary measures and that a definition based upon FTLE

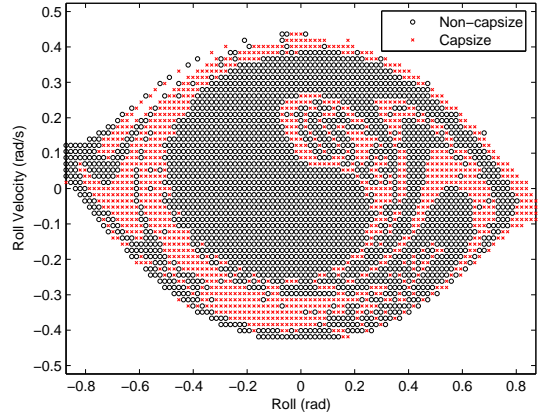


Figure 8: Safe basin indicating non-capsizing and capsize in random seas for those cases capsizing after one excitation period.

methods could provide a conservative indicator of capsizing.

3 Random Seas

3.1 Random seas: modelling details

In random seas, the term $M(t)$ in Equation 2 is written as Equation 5 (Senjanović *et al.*, 2000; Gu, 2004)

$$M(t) = I\alpha_0\omega_n^2 \frac{\sqrt{2}d\omega}{g} \sum_{i=1}^N (\omega_i)^2 \sqrt{S(\omega_i)} \sin(\omega_i t + \epsilon_i) \quad (5)$$

where $N = 180$ is the number of wave components, $d\omega = 0.0083$ rad/s is the size of the wave frequency increment, ω_i is the encounter frequency for each wave component, ϵ_i is a random phase angle between 0 and 2π for each wave component, and $S(\omega)$ is a wave energy spectrum. For this study the ISSC two-parameter spectrum, Equation 6 was used with a significant wave height $H_s = 4.94$ m and characteristic frequency $\omega_z = 0.527$ rad/s for consistency with Section 2.

$$S(\omega) = 0.11H_s^2 \frac{\omega^4}{\omega^5} \exp\left(-0.44\left(\frac{\omega_z}{\omega}\right)^4\right) \quad (6)$$

Details as to the derivation of Equation 5 can be found in Senjanović *et al.* (2000), Jiang *et al.* (1996), and Chapter VIII of *Principles of Naval Architecture* (1989). A sample safe basin representing the simulation of Equations 2 and 5 is presented in Figure 8. In Figure 8 the same random seed is used

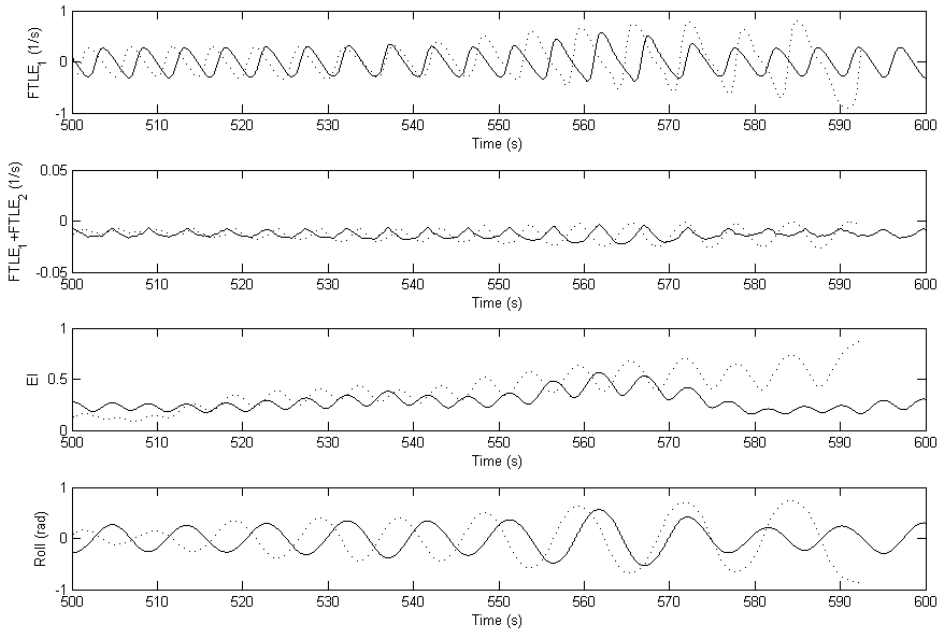


Figure 9: $FTLE_1$ (top), sum of FTLE (middle top), EI (middle bottom), and roll (bottom) for *Edith Terkol* in random beam seas. Both cases correspond to initial conditions $\phi = 0$ rad, $\dot{\phi} = 0$ rad/s. Dotted and solid lines denote capsizes and non-capsizes respectively.

for each simulation, therefore each initial condition pair is subject to the same random wave time series.

3.2 Random seas: finite-time Lyapunov exponents

In random seas, finite-time Lyapunov exponents and energy index values were calculated via simulation for the numerical model of the *Edith Terkol* given by Equations 2 and 5. Figure 9 compares data for two time series with identical initial conditions in random seas in which one case leads to capsizes, and one non-capsizes. As in Figures 4-5, EI values serve as a reflection of the roll time series behavior. Conversely, the finite-time Lyapunov exponent time series demonstrates distinct variations in behavior well before the point of capsizes.

For example, after approximately 540 seconds of simulation, there is a marked phase change between capsizes and non-capsizes FTLE time series in which the run leading to an ultimate state of capsizes changes from leading to lagging the non-capsizes time series. Additionally, the $FTLE_1$ values increase substantially at approximately 550 seconds of simulation. In consideration of the sum of the two FTLE for both capsizes and non-capsizes

runs, it is found that over the entire simulation time the maximum value for $FTLE_1 + FTLE_2$ for the capsizes case is positive, 0.0028 while it is -0.0028 for the non-capsizes case. This again lends validity to the belief that quantitative indicators of capsizes can be formulated via the use of the FTLE as well as that the FTLE holds promise as an indicator of periods of coming quiescence.

Figure 10 shows histograms of the maximum first FTLE for capsizes and non-capsizes cases in random seas. Only those runs capsizing after one excitation cycle are considered as established in Section 2. In Figure 10, similar to Figure 1, those runs resulting in capsizes typically experienced larger maximum FTLE. Also shown in Figure 10 is the cycles from the occurrence of the peak FTLE to capsizes. While in random seas, the cycles to capsizes is dependent upon the random seed in the phase term of the wave train, it is apparent for the sample set presented herein, that for many cases capsizes occurs sufficiently long after the peak in the FTLE time series that corrective measures could be implemented.

Figures 11-12 plot histograms and state space of the entropy rate-like value summing the two finite-time Lyapunov exponents. Those runs which capsizes after one excitation cycle have, on average,

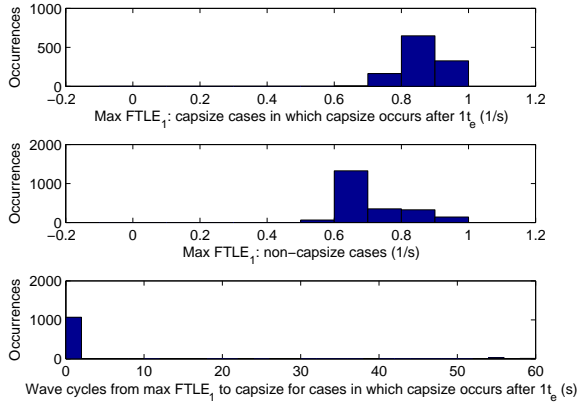


Figure 10: Histograms of maximum $FTLE_1$ for capsize (top) and non-capsize (middle) cases in random seas as well as cycles from maximum $FTLE_1$ to capsize (bottom).

a positive maximum $FTLE_1 + FTLE_2$ while those runs which do not capsize tend toward negative values as shown in Figure 11. As seen in Figure 12 those non-capsize cases with positive maximum $FTLE_1 + FTLE_2$ often lie on the fractal boundaries between capsize and non-capsize. Measures detecting positive, or small negative values of the sum of all Lyapunov exponents, in addition to detecting peaks, phase differences, and other oddities in the FTLE time series, can indicate impending capsize.

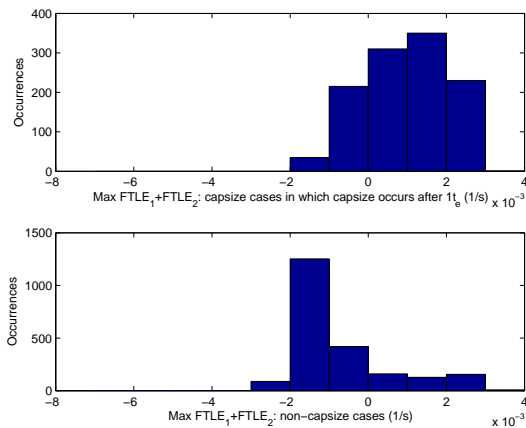


Figure 11: Histograms of maximum $FTLE_1 + FTLE_2$ for capsize and non-capsize cases in random seas.

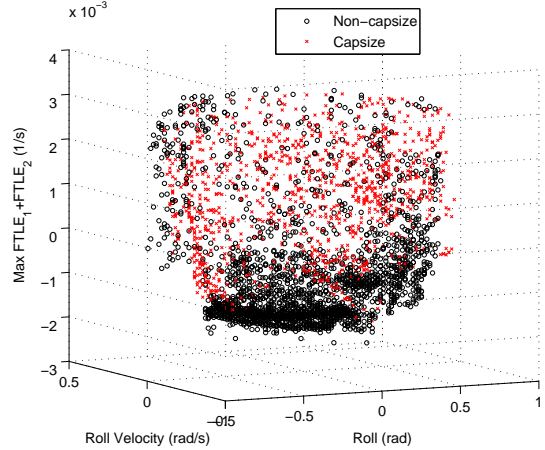


Figure 12: 3-dimensional plot of initial conditions and maximum $FTLE_1 + FTLE_2$ for capsize and non-capsize cases in random seas.

4 Conclusions

Based upon numerical simulation of Soliman and Thompson's (1991) simplified single degree of freedom roll motion model, this work demonstrates that finite-time Lyapunov exponent calculations provide viable indicators of impending capsize in both regular and random seas. Instabilities leading to capsize are detected through:

1. peaks in the FTLE time series,
2. time series phase changes and/or other qualitative idiosyncratic behavior, and
3. positivity of the sum of the FTLE spectrum in time.

This further supports the conclusions arrived at by McCue and Troesch in their studies of three-degree of freedom numerical and experimental results (2004; 2005).

To implement this theory in a practical, on-board manner, a number of areas for future research arise. Specifically, it would be of use to further study the feasibility of this technique in detecting quiescence as applied to ship based aviation applications via comparison of results from both methods for ship motions in six degrees of freedom. Colwell expressed concern that a scalar representation of the ship motion environment obscures some of the understanding of the limiting aspects of sea-air operations (2002a). It is the author's belief that a mathematical approach, such as that presented by finite-time Lyapunov exponents, enables understanding of the fundamental physics of the system

while still reaping the benefits of a scalar output.

Additionally, more quantitative means to detect variations in the FTLE time series are required. It is not always practical, feasible, or computationally efficient to calculate the entire FTLE spectrum, and thus measuring for positivity of the sum of the finite-time exponents may not be the ideal quantitative indicator. Instead, benchmarks for peak values and techniques to quantify phase and other behavior changes in the $FTLE_1$ time series must be developed through further simulation and analysis of experimental data for a range of hull forms in realistic seas.

5 Acknowledgements

This research was conducted while funded by the ONR-ASEE Summer Faculty Research Program. Additionally, the author wishes to thank William Belknap (Seakeeping Division, Code 5500, NSWC-CD), Judah Milgram (Sea-Based Aviation, Code 5301, NSWC-CD), and Armin Troesch (University of Michigan) for their assistance and insights on this topic.

References

- Arnold, L., Chueshov, I., & Ochs, G. 2003. *Stability and capsizing of ships in random sea-a survey*. Tech. rept. 464. Universität Bremen Institut für Dynamicsche Systeme.
- Beck, Robert F., Cummins, William E., Dalzell, John F., Mandel, Philip, & Webster, William C. 1989. Motions in Waves. *Chap. VIII of: Lewis, Edward V. (ed), Principles of Naval Architecture*. Society of Naval Architects and Marine Engineers.
- Benettin, Giancarlo, Galgani, Luigi, Giorgilli, Antonio, & Strelcyn, Jean-Marie. 1980. Lyapunov characteristic exponents for smooth dynamical systems and for Hamiltonian systems; a method for computing all of them. *Meccanica*, 9–20.
- Colwell, J.L. 2002a (May). Maritime Helicopter Ship Motion Criteria-Challenges for Operational Guidance. *In: NATO RTO SCI-120 Symposium on "Challenges..."*.
- Colwell, J.L. 2002b. Real time ship motion criteria for maritime helicopter operations. *In: ICAS 2002 Congress*.
- Eckhardt, Bruno, & Yao, Demin. 1993. Local Lyapunov exponents in chaotic systems. *Physica D*, **65**, 100–108.
- Falkovich, Gregory, & Fouxon, Alexander. 2004. Entropy production and extraction in dynamical systems and turbulence. *New Journal of Physics*, **6**(50).
- Falzarano, Jeffrey M. 1990. *Predicting complicated dynamics leading to vessel capsizing*. Ph.D. thesis, University of Michigan.
- Ferrier, B., & Manning, T. 1998. Simulation and testing of the landing period designator (LPD) helicopter recovery aid. *Naval Engineers Journal*, **110**(1), 189–205.
- Ferrier, B., Baitis, A.E., & Manning, A. 2000a. Evolution of the Landing Period Designator (LPD) for Shipboard Air Operations. *Naval Engineers Journal*, **112**(4), 297–315.
- Ferrier, Bernard, Applebee, Terrence, Manning, Anthony, & James, David. 2000b (May). Landing period designator visual helicopter recovery aide; theory and real-time application. *In: Proceedings of the 56th Annual Forum of the American Helicopter Society*.
- Francescutto, Alberto, & Serra, Andrea. 2002. Experimental tests on ships with large values of B/T, OG/T and roll period. *In: 6th International Ship Stability Workshop*.
- Gu, Jia-Yang. 2004. Nonlinear rolling motion of ship in random beam seas. *Journal of Marine Science and Technology*, **12**(4), 273–279. National Taiwan Ocean University, publisher.
- Jiang, Changben, Troesch, Armin W., & Shaw, Steven W. 1996. Highly nonlinear rolling motion of biased ships in random beam seas. *Journal of Ship Research*, **40**(2), 125–135.
- McCue, Leigh S. 2004. *Chaotic vessel motions and capsize in beam seas*. Ph.D. thesis, University of Michigan.
- McCue, Leigh S., & Troesch, Armin W. 2004 (November). Use of Lyapunov exponents to predict chaotic vessel motions. *In: 7th International Ship Stability Workshop*.
- McCue, Leigh S., & Troesch, Armin W. 2005. A combined numerical-empirical method to calculate finite time Lyapunov exponents from experimental time series with application to vessel capsizing. Under review, *Ocean Engineering*.

- Murashige, S., Yamada, T., & Aihara, K. 2000. Nonlinear analyses of roll motion of a flooded ship in waves. *Philosophical Transactions of the Royal Society of London A*, **358**, 1793–1812.
- Murashige, Sunao, & Aihara, Kazuyuki. 1998a. Co-existence of periodic roll motion and chaotic one in a forced flooded ship. *International Journal of Bifurcation and Chaos*, **8**(3), 619–626.
- Murashige, Sunao, & Aihara, Kazuyuki. 1998b. Experimental study on chaotic motion of a flooded ship in waves. *Proceedings of the Royal Society of London A*, **454**, 2537–2553.
- Nayfeh, A.H., & Khdeir, A.A. 1986. Nonlinear rolling of ships in regular beam seas. *International Shipbuilding Progress*, **33**(379).
- Nayfeh, A.H., & Sanchez, N.E. 1990. Stability and complicated rolling responses of ships in regular beam seas. *International Shipbuilding Progress*, **37**(412), 331–352.
- O'Reilly, Peter J.F. 1987. Aircraft/deck interface dynamics for destroyers. *Marine Technology*, **24**(1), 15–25.
- Papoulias, Fotis Andrea. 1987. *Dynamic analysis of mooring systems*. Ph.D. thesis, Department of Naval Architecture and Marine Engineering, University of Michigan, Ann Arbor, MI.
- Senjanović, I., Ciprić, G., & Parunov, J. 2000. Survival analysis of fishing vessels rolling in rough seas. *Philosophical Transactions of the Royal Society of London A*, **358**, 1943–1965.
- Soliman, Mohamed S., & Thompson, J.M.T. 1991. Transient and steady state analysis of capsizing phenomena. *Applied Ocean Research*, **13**(2).
- Spyrou, K.J. 1996. Homoclinic connections and period doublings of a ship advancing in quartering waves. *Chaos*, **6**(2).
- Wolf, Alan, Swift, Jack, Swinney, Harry, & Vastano, John. 1985. Determining Lyapunov exponents from a time series. *Physica D*, **16**, 285–317.